An investigation into the effect of CoCrMo powder characteristics on the powder bed density in laser-based powder bed fusion units

Cornelius P. Kloppers
School of Mechanical and Nuclear Engineering – Additive Manufacturing Research Group, North-West University – Potchefstroom Campus, Potchefstroom, South Africa, and

Deon J. de Beer
Centre for Rapid Prototyping and Manufacturing, Central University of Technology Free State, Bloemfontein, South Africa

Abstract

Purpose – The increased use cases for laser powder bed fusion (LPBF) in the research and commercial domains necessitate a better understanding of the inputs and the processing parameters. Porosity in parts manufactured by LPBF could lead to premature failure and increased cost. The powder bed, which is selectively laser melted, must be as densely packed as possible to ensure high-density parts. This paper aims to identify and qualify the variables that affect the packing density of the powder bed.

Design/methodology/approach – Six different independent variables that affect the packing density of the powder were identified and quantified. The chemical composition, true powder density, powder size distribution, powder circularity and convexity and powder morphology were studied. A powder bed density capsule was printed in place to determine the actual powder bed density in the LPBF unit.

Findings – Particle size destitution is the most critical aspect of the packing density in the LPBF unit. Powder with better circularity, convexity and higher powder density has proven to pack less densely than powder with many smaller particles. A more significant number of fine particles will ensure the voids between larger particles are filled, and a denser item, with less porosity, can be manufactured.

Originality/value – The independent variables quantified in this study to determine their effect on the packing densities are discussed. Adherence to the ASTM standard applicable to this industry is discussed, and the quantification method is evaluated. This work's original contribution is identifying the effect of the ratio of D_{90} to D_{10} values based on particle diameter and its interaction within the LPBF unit to result in the highest possible packing density.

Keywords Laser powder bed fusion, CoCrMo, Powder bed density

Paper type Research paper

1. Introduction

Additive manufacturing (AM) has become a widely used technique in both research and commercial environments, with metal additive manufacturing (MAM) being particularly popular (Auricchio and Marconi, 2016).

The unique advantages of AM, such as conformal applications and the ability to reduce energy reliance on fossil fuels, have made it an attractive option for novel applications such as flexible hybrid electronics and the production of semiconductor photocatalysts (Hu *et al.*, 2023; Bai *et al.*, 2023). In addition, AM has been used as an assistive technology to enhance mass production manufacturing methods, such as injection moulding, by implementing conformal cooling (Shinde and Ashtankar, 2017).

Despite the widespread use of AM, the quality and functionality of the part produced depend heavily on the manufacturing process parameters (Zhao *et al.*, 2023). In laser-based powder bed fusion, metal powder is selectively melted layer-by-layer to fabricate the desired parts (Abdulhameed *et al.*, 2019). The thickness of these layers, known as the layer height, varies across different AM units, and the density of the powder bed is crucial to avoid porosity in the final product (Townsend *et al.*, 2016; Zhang *et al.*, 2023).

The powder morphology also plays a critical role in the mechanical properties of the parts produced (Cacace and Semeraro, 2020; Slotwinski and Garboczi, 2015; Spierings

The current issue and full text archive of this journal is available on Emerald Insight at: **https://www.emerald.com/insight/1355-2546.htm**

Rapid Prototyping Journal
30/11 (2024) 335–343
Emerald Publishing Limited [ISSN 1355-2546]
[DOI 10.1108/RPJ-01-2024-0027]

The Authors would like to acknowledge the funding received from the Department of Science and Innovation (DSI) in South Africa, for funding this research through the Collaborative Program in Additive Manufacturing (CPAM).

Received 17 January 2024
Revised 9 May 2024
4 July 2024
Accepted 4 October 2024

et al., 2011; Tan *et al.*, 2017). Powder characteristics, such as chemical composition, particle shape and particle size distribution, can all influence the final product quality (Slotwinski and Garboczi, 2015). To ensure high-quality parts, it is essential to have a thorough understanding of the powder characteristics and their influence on the behaviour of the laser-based powder bed fusion unit. However, accurately measuring these input parameters requires sophisticated equipment (Slotwinski and Garboczi, 2015).

Several studies have shown that true powder density measurements; scanning electron microscopy (SEM); feedstock powder chemical composition and particle shape analysis; and size distribution are valuable tools for characterising powders used in MAM (Averardi *et al.*, 2020). For instance, medical-grade CoCrMo has a specific chemical composition that must conform to ASTM standard F75 (ASTM, 2017), and evaluating commercially available CoCrMo powders is necessary to determine their suitability for laser-based powder bed fusion production of implants (Saha and Roy, 2022).

This study aimed to investigate the influence of powder characteristics on the packing density within the AM powder bed, focusing on commercially available CoCrMo powders. By quantifying these input parameters and understanding their effects on the system behaviour, this study hoped to improve the adoption of AM in the industry and achieve the best possible part quality in laser-based powder bed fusion production of metallic parts.

2. Materials and methods

With AM, and more specifically laser-based powder bed fusion, being a new technology, suppliers of ASTM F75 powders are limited, especially outside the European and American markets. The three most easily obtainable and the highest quality CoCrMo powders were procured for this study. Using three different powders ensured that the knowledge gained from this empirical study was not limited to a single manufacturer or powder type. Preservation of anonymity is critical to remain unbiased. The powders were, therefore, referred to as powders A, B and C. These powders are advertised as ASTM F75 compatible powders and are applicable in the dental and broader medical industry when parts are produced using AM. All the quantified parameters of each powder were compared.

Feedstock powder chemical composition was determined by inductively coupled plasma-optical emission spectroscopy (ICP-OES) and provided detailed weight percentage data regarding the powder's chemical composition. Comparison between the powders' chemical composition and the ASTM F 75 standard yielded results regarding conformity to the standard. An AccuPyc 1340 Pycnometer was used to measure the apparent density. The powders were dried at 120°C, then each sample was weighed, and the dry powder was poured into a 3.5 cm^3 sample cell. The weight recorded for each sample was between 4.9 g and 5.0 g. Powders were analysed three times, and an average of the three analyses was taken as the powder density. A Malvern Morphologi 4 static automated imaging machine was used to analyse the particle size distribution and the particle morphology of the three powders. In addition, a SEM (FEI Quanta FEG 250 SEM) was used to evaluate the morphology of powder particles.

Finally, the powder bed density was determined in the Coherent Creato commercial AM unit used in this study. Printing parameters used during the manufacturing of these samples were the laser power of 165 W with a 50% overlap in hatching, the marking speed which was set to 630 mm/s, and a laser spot size of 40 μm. A 67-degree hatch rotation with a zig-zag pattern was used with an offset of 80 μm to the boundary. The methodology described by Jacob *et al.* (2016) was used to yield repeatable results. All tests were carried out in triplicate, and the exact geometry of the enclosed cell units, as developed by Jacob *et al.* was used. Figure 1 illustrates the enclosed cell units used to determine the powder bed density.

Each capsule manufactured had the support material removed and was then weighed five times on an analytical lab balance accurate and repeatable to 0.1 mg, and the average weight was then calculated. The cap was removed, and where possible, this was also saved and weighed; the powder was then removed, and the container was flushed with both water and IPA, consecutively, using a syringe to ensure all powder particles were removed. Finally, compressed air was also used to ensure an empty capsule. The capsule was then dried for 12 h at a temperature of 120°C to remove all moisture that could affect the weight of the capsule. The capsule was then filled with distilled water in a temperature-controlled environment for 24 h to ensure a stable temperature. The temperature was also noted for density calculations. Each capsule was then weighed before and after the addition of the water to determine the volume of the capsule as accurately as possible.

With the quantification of the powder bed density and the physical and measurable properties of the powders mentioned above, an analysis can be conducted into the effect of each of these parameters on the packing density of the powder in the AM unit.

3. Results and discussion

3.1 Chemical composition

ICP-OES is the recommended method to determine the chemical composition according to ASTM F3049-14 (Einhauser, 1997). The results obtained in this analysis provide insight into the weight percentage of each element in the metal alloy. As a control, the ASTM F75 standard was used to evaluate the weight percentage of the elements present. The results from the ICP-OES are presented in Table 1.

The ASTM F75 standard provides an upper and lower limit for material elemental composition to adhere to. All elements marked in red are outside the specified range and N/D indicates elements that were not detected. The results for Powder A indicated that all the elements were detected within the range specified by the standard. Powder A contained the highest percentage of chromium and manganese, still within the specified range. Carbon, tungsten, phosphorous, sulphur, nitrogen and boron were undetected. These elements have a lower limit of 0% and are not required to be present in the alloy. The standard does not refer to calcium but calcium made up 0.08% by weight of the sample.

The results for Powder B were very similar to Powder A, but silicon was detected in amounts above the upper limit as

Figure 1 Enclosed cell unit manufactured for powder bed density evaluations

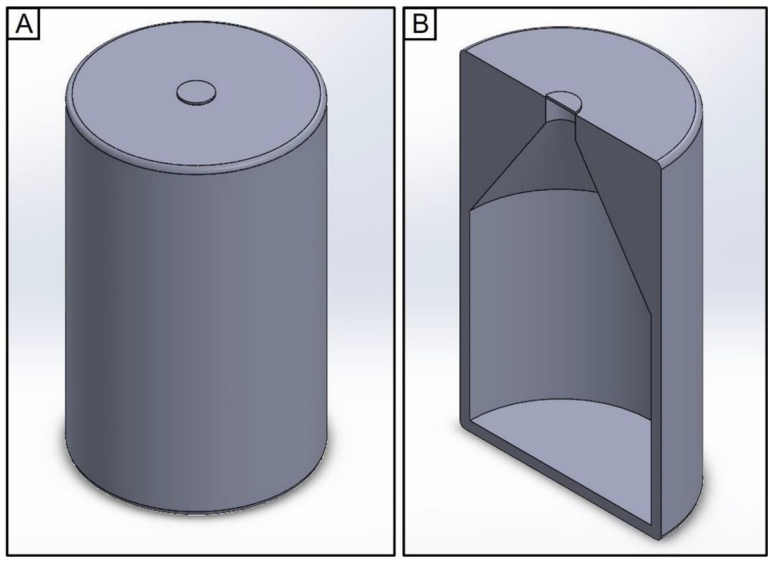

Note: (a) Overall sample design; (b) cross-sectional view of the enclosed cell unit
Source: Figure by authors

Table 1 ASTM F-75 specification of CoCrMo and the chemical composition of powder A, B and C

Element	ASTM F-75 specification Min %	Max %	Powder 1 % Present	Powder 2 % Present	Powder 3 % Present
Cobalt	68.00	58.71	63.40	65.70	62.80
Chromium	27.00	30.00	29.00	27.10	28.70
Molybdenum	5.00	7.00	5.32	5.33	6.25
Nickel	0.00	0.50	0.11	0.04	0.25
Iron	0.00	0.75	0.47	0.04	0.47
Carbon	0.00	0.35	N/D	N/D	N/D
Silicon	0.00	1.00	0.56	1.07	0.50
Manganese	0.00	1.00	0.29	0.01	0.15
Tungsten	0.00	0.20	N/D	N/D	N/D
Phosphorous	0.00	0.02	N/D	N/D	N/D
Sulphur	0.00	0.01	N/D	N/D	N/D
Nitrogen	0.00	0.25	N/D	N/D	N/D
Aluminium	0.00	0.10	0.07	0.07	0.12
Titanium	0.00	0.10	0.01	0.01	0.01
Boron	0.00	0.01	N/D	N/D	N/D
Calcium	0.00	0.00	0.08	0.08	0.10

Note: N/D for not detected and red indicates outside the allowable range
Source: Table by authors

specified by the standard. Gravimetrically, Powder B had the highest percentage of cobalt, the primary alloying element present, with 2.3% more cobalt than Powder A and 2.9% more cobalt than Powder C. Due to the high cobalt content, this powder had the lowest percentage of chromium present, together with nickel, iron and manganese. The silicon in Powder B exceeded the prescribed amount by 0.07%; thus, the powder did not adhere to the ASTM F75 standard.

Powder C had the highest percentage of molybdenum, with 0.93% more than Powder A and 0.92% more than Powder B. Molybdenum is the most expensive alloying element present in this alloy and should produce enhanced high-temperature behaviour due to the refractory properties of molybdenum. In the case of Powder C, the aluminium content exceeded the prescribed amount, therefore, this powder did not adhere to the standard.

Based on the ICP-OES results, as measured by the gravimetric percentage of each element inside an alloy, it would be logical to assume that the weight percentages determined by the ICP-OES process will accumulate to 100.00%. This was not the case, with the accumulation of elemental composition accounting for only 99.31% in Powder A, 99.45% in Powder B and 99.35% in Powder C. The data provided by the test facility has data accurate only to the second decimal place and this could, in theory, be a rounding error. Fontoura *et al.* (2022) proposed the use of microwave-induced plasma OES (MIP-OES) as an alternative to ICP-OES, specifically for trace element analysis. They found that plasma diagnostic strategies, as well as calibration methods and sample preparation, play a significant role in the OES process and results.

The three powders present conform, to a considerable extent, to the prescribed ASTM F75 standard, and the elements in Powder B and Powder C, which are outside the limits proposed by the standard, are marginal. These powders would, in all likelihood, be safe for surgical implants as specified by the standard.

3.2 Particle size distribution and powder morphology

Automated imaging provides valuable insight into the particle size and the morphology of the powder. The central aspect that the automated imaging provides is a detailed report of the powder circularity, diameter, and convexity. Each powder had three sample measurement batches, with the average of all three tests presented in Table 2. This experiment analysed a total of 163,940 particles over a total of 9 automated imaging tests.

Powder circularity is a measure of the actual perimeter length of the particle divided by the theoretical circumference of a circular particle with the same surface area as that of the measured particle. Using gas-atomised powders in the AM process, most particles should be circular when observed in a two-dimensional manner.

Powder size gauges regarding circularity, diameter and convexity are evaluated by denoting each property's D_{10}, D_{50} and D_{90} values. The sizing gauge D_{10} indicates that 10% of the powder sample is less than the stated value; D_{50} is the median value and denotes that 50% of the particles are below the stated value; and D_{90} states that 90% of the particles in the specific sample are smaller than the stated D_{90} value.

The circularity D_{90} values indicate that Powder A consists of the most circular particles, followed closely by Powder B (0.1% variation) and Powder C (0.4% variation). The median particle circularity of the powders has a wider distribution, with Powder B having the most circular median particle by 0.8% compared to Powder A. When a comparison of Powder B and Powder C is considered, a 3.1% variation is present. The D_{50} values continue the trend in the median values, with Powder B having the most circular particles, followed by Powder C and Powder A. Although Powder A has the highest D_{90} values, Powder B has consistently higher values when the other circularity gauges are considered, as irregularly shaped particles could cause imperfections in the powder bed of an AM unit. Powder B was shown to have the best circularity characteristics.

Powder diameter plays an essential role in the packing density of the particles in the AM unit. The smaller the particles, the smaller the unoccupied spaces between particles. The spread of particle sizes also plays a critical role. The finer the particles in a powder, the fewer unoccupied spaces will be left and, in theory, the higher the powder bed density should be.

When consideration is given to the smallest 10% of the particles (the D_{10} values), Powder A is only 62.7% the size of Powder C, with the Powder B D_{10} value falling between these values. The median values of Powder A and Powder B are relatively close (57.8%), with Powder C being significantly larger (68.9%). Although Powder A had the best D_{10} values, Powder B far surpasses it when considering the D_{50} and D_{90} results. Powder B has a D_{90} value 19.8% less than Powder A and a value which is 42.5% less than Powder C.

The inclusion of many very fine particles in Powder A should yield a good pacing density of the AM unit, as these fine particles can fit between the larger particles. However, this is not an absolute result, as the ratio of the particle sizes will also play a significant role when the ultimate packing density in the powder bed of the AM unit is considered. Powder A has a low D_{10} value but a significantly larger D_{90} value. The ratio of these values is 3.948 for Powder A, 2.560 for Powder B and 2.579 for Powder C. This size ratio will have an impact when the effect of particle size distribution is considered on the packing density. This ratio can also be used to indicate the quality of the manufacturer's process when manufacturing these powders. A narrow spread or a lower ratio of sizes indicates better control over their manufacturing processes.

Table 2 Results of powder characteristics

+	Circularity			Diameter			Convexity		
Powder	**A**	**B**	**C**	**A**	**B**	**C**	**A**	**B**	**C**
Min.	0.079	0.1297	0.199	0.540	0.697	0.590	0.507	0.582	0.580
Max.	1.000	1.0000	1.000	85.180	79.063	83.290	1.000	1.000	1.000
Mean	0.905	0.9117	0.893	20.143	18.963	28.920	0.981	0.983	0.977
D_{10}	0.720	0.7520	0.744	8.877	11.420	16.157	0.935	0.949	0.945
D_{50}	0.954	0.9617	0.932	17.853	16.687	28.187	0.990	0.992	0.986
D_{90}	0.993	0.9920	0.989	35.047	29.243	41.677	0.998	0.998	0.997
STDV	0.127	0.1163	0.115	10.637	7.880	10.360	0.036	0.031	0.032
RSD %	0.140	0.1275	0.129	0.525	0.416	0.360	0.363	0.032	0.033
No. of particles	67,994	70,911	25,035	679,940	70,911	25,035	67,994	70,911	25,035

Source: Table by authors

Powder convexity is the measure of the edge circularity of the particles. The closer the values are to unity, the more circular the particles are, with a perfect circle having a convexity of 1. The minimum values in all three powders presented have an average convexity of 0.5565, with Powder A having significantly lower convexity than the other two powders. All the powders have theoretically circular particles present with a maximum value of 1 for all the powders. When considering the D_{10} values, Powder A had the lowest quality in terms of convexity, with a 2.5% lower convexity than Powder B and 1.1% less than Powder C. This correlates well with the statement that the narrower the spread of the particle size, the better the quality control of the manufacturing process seems to be. The low convexity of powder A indicates more elongated grains; although the particles are small, they are oddly shaped.

The values obtained from the automated imaging process can be validated by SEM; although a total of 163,940 particles were evaluated for the results in Table 2, a much smaller sample should show the same trends when captured in the micrographs shown in Figure 2.

Micrographs of Powder A can be seen in Figures 2(a) and (b). Figure 2(a) provides a general overview of the significant variation in particle shape and size that can be observed. Many particles have satellites present on the particles and have a distorted shape. In Figure 2(b), a notable number of tiny particles is visible, and particles are present that are not spherical and are severely distorted. Micrographs of Powder B [Figure 2(c) and Figure 2(d)] show a more consistent spread of particles that are more uniform in size and shape when compared to Powder A. Although a significant number of satellites can be seen on this powder, very few irregularly

Figure 2 Micrograph of powder particles of all three powders. A consistent imaging scheme to facilitate comparison was used where 300 μm and 50 μm of each sample were taken

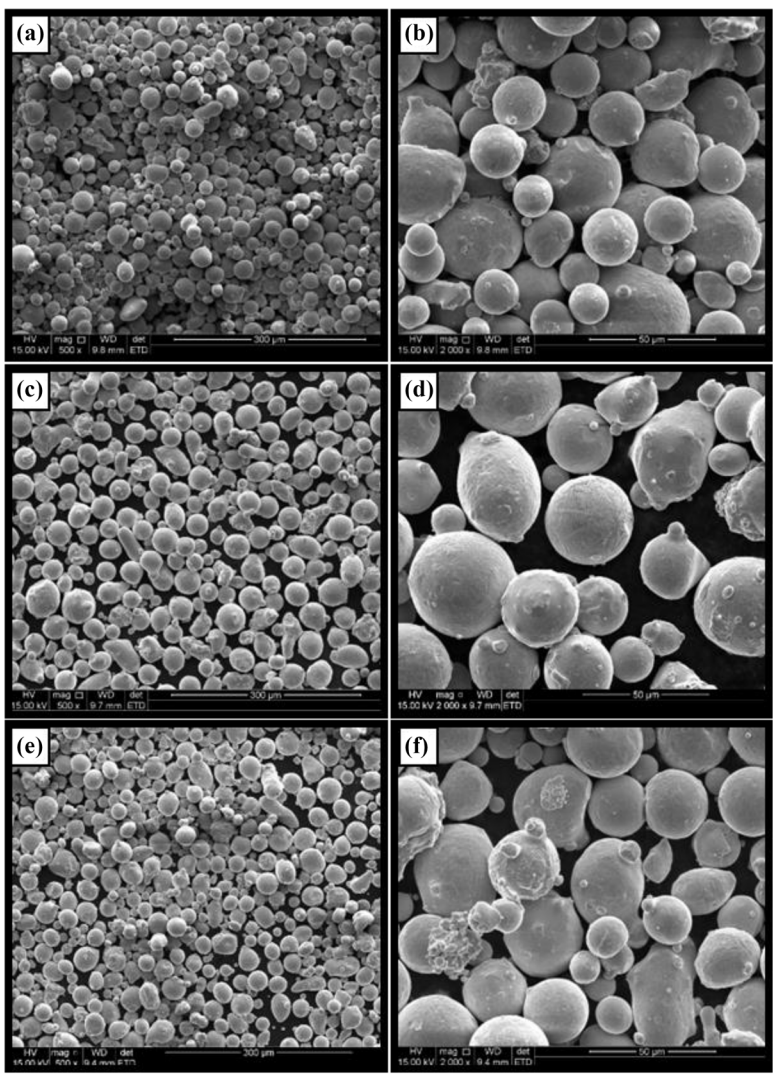

Notes: (a); (b) are images of Powder A; (c); (d) are images of Powder B. (e); (f) are images of Powder C
Source: Figure by authors

shaped particles can be seen, except for a few elongated particles.

The automated imaging results micrographs of Powder C [Figure 2(e) and Figure 2(f)] show, as expected, better groupings of particle sizes. This powder had the worst circularity and convexity, which is also evident in the images in Figure 2. The micrographs show several randomly shaped particles; the spherical powder particles that are present seem to have fewer satellites than Powder B.

3.3 Powder density

Helium pycnometry was used to obtain the true density of each powder. During the pycnometry process, the powder is immersed in helium, and the density can be determined by Boyle's law. This process does not account for the internal porosity of the powder that could have formed during the manufacturing process. Helium pycnometry results are shown in Table 3.

Helium pycnometry was conducted under very similar conditions with less than 0.2°C variation between the tests and only a 5.23% (26 mg) difference in the weight of the powder that was evaluated. Powder B achieved the highest density alongside the smallest standard deviation; the standard deviation of this powder is more than an order of magnitude lower than that of the other powders. Powder C had a lower density than Powder B, and Powder A had a significantly lower density than either Powder B or C.

The true powder density of these different CoCrMo powders is expected to vary as the chemical composition of the powders differs. Internal powder porosity can have a telling effect on the density of the powder; this can, however, not be quantified by the internal porosity enclosed inside the very fine particles. The more internal porosity prevalent in the powder, the worse the powder will perform when used inside an AM unit as the alloy is melted and the gas trapped between the powder particles will escape and could lead to porosity inside the parts produced.

3.4 Powder bed density

The powder bed density in a commercial AM unit is one of the critical variables that determines the quality of the parts produced by the laser-based powder bed fusion process. The powder bed density has a direct impact on the porosity present inside the parts produced, and this, in turn, has a significant effect on the strength and fatigue life of the parts produced by AM. Therefore, powder bed density plays a significant role in the viability of AM as a manufacturing technology. The methodology of Jacob *et al.* (2016) was used and carried out in triplicate to ensure repeatable results, as shown in Table 4.

For Powder A, the internal water volume for each capsule had a maximum variation of 0.1889 mL between Capsules 1 and 3. The difference can be attributed to the manual filling process of each container and imperfections in the manufacturing process. The effective material density of the three containers showed minimal variation. With only 0.00275 g/mL between the three capsules, this indicates that the results obtained are within the repeatability window. An average powder bed density of 62.8794% was obtained for this powder, with only a 0.033% variation between the three different capsules.

Powder B showed a significant variation between the three different capsules. Capsule 2 had a significantly larger cavity volume with 0.2209 mL more water capacity than Capsule 3. Both Capsule 1 and Capsule 3 presented powder bed densities that are similar, with Capsule 2 being an outlier with a maximum variation of 0.26% between Capsule 2 and Capsule 3. A powder bed density of 59.54% was obtained for Powder B.

Powder C had an average internal cavity volume of 5.7897 mL with a variation of 0.2134 mL between the different capsules. Although the effective material density in the powder bed is below the 5.00 g/mL seen in Powder A and Powder B, the results for Powder C proved repeatable. Even though the effective material density is the lowest of all three samples, the powder bed density is 60.0817%. This is due to the true powder density of Powder C obtained by Helium pycnometry analysis that was used as a reference value when the density was calculated.

As regards the elemental composition of three commercial powders advertised as ASTM F75 compatible powders, the results indicated that these powders comply with the standard with most elements present within these powders. Powder A complies fully with the standard, with Powder B the only powder that lies outside the tolerance of the standard with 0.02% more Silicon than recommended. Powder C lies on the

Table 3 Helium pycnometry results

Quantifiable property	Powder A	Powder B	Powder C
Sample mass [g]	4.9987	5.0082	4.9821
Temperature [°C]	17.42	17.29	17.18
Expansion volume [cm^3]	8.4676	8.4676	8.4676
Cell volume [cm^3]	5.7679	5.7679	5.7679
Sample density [g/cm^3]	8.1717	8.4440	8.3039
Density standard deviation [g/cm^3]	0.0034	0.0003	0.0092

Source: Table by authors

Table 4 Powder bed density results

Sample #	Internal water volume (mL)	Effective material density (g/mL)	Powder bed density (%)
Powder A			
Sample 1	5.7077	5.1390	62.8878
Sample 2	5.7958	5.1366	62.8583
Sample 3	5.8966	5.1393	62.8920
Average	5.8000	5.1383	62.8794
Powder B			
Sample 1	5.7947	5.0346	59.6239
Sample 2	5.9212	5.0134	59.3727
Sample 3	5.7003	5.0354	59.6339
Average	5.8054	5.0278	59.5435
Powder C			
Sample 1	5.7873	4.9972	60.1788
Sample 2	5.6842	4.9803	59.9745
Sample 3	5.8976	4.9899	60.0907
Average	5.7897	4.9891	60.0817

Source: Table by authors

extreme value of the powder tolerance regarding Aluminium. The powders presented here yielded good conformity to the standard and should be safe for the uses stipulated in the standard. Variations in measurements within the ICP-OES and the possibility of applying MIP-OES in future to obtain better scanning for trace elements should yield more definitive results. The powders performed as expected and complied with the ASTM F75 standard for chemical composition. These powders should be safe for use in the manufacture of medical-grade implants.

Particle size distribution and powder morphology significantly affect the powder's packing density in the powder bed and the density of the final parts produced by the AM process [10]. The three gas-atomised powders used in this study were expected to contain non-spherical particles due to the nature of the gas-atomisation manufacturing process. The results from automated imaging and SEM micrographs proved that better results were achieved than water atomisation, but worse than plasma atomisation, as would be expected [14,15]. Interestingly, in most cases, the particle size distribution was lower than specified by the manufacturer at both the upper and lower limits. The exception was Powder C, which contained D_{90} values of 6.677 μm larger than specified.

The powder bed density is a percentage value of how densely particles pack compared to the measured true density determined by helium psychometry. The changes in density could be attributed to two different factors; firstly, variations in chemical compositions and the variation of the chemical composition of the different powders can have a significant effect on the density as an increase in heavy elements could result in higher density. The second factor is internal porosity due to the gas atomisation manufacturing process. This could also drastically affect the density measurement. Surface porosity will play no role as the helium will fill the voids during pycnometry. If powders contain internal porosity, this will skew the results of the powder bed density. As seen in the helium pycnometry results, Powder B has a significantly higher density than Powder A and Powder C.

Eliminating the porosity in the powder one particle at a time is not feasible due to the number of particles and the particle size. A possible approach can be followed if the theoretical 100% dense powder density can be calculated from the chemical composition measured by the ICP-OES process. When the weight percentages and elemental densities are used to calculate the density, Powder A yields a value of 8.3535 g/mL, with Powder B 8.3736 g/mL and Powder C 8.3038 g/mL. With these new values, the powder bed density would be 61.5109% for Powder A, 60.0437% for Powder B and 60.0906% for Powder C.

As shown in this study, numerous factors influence the packing density of the particles in the powder bed, and to obtain the most commercially viable results in part properties it would be advantageous to have a dense possible packing of the powder. The quantification of these results has shown that the particle size distribution has the most significant effect on the packing density. The result of this study implies that the industry standard for particle size distribution, which is typically between 15 μm and 45 μm, does not yield the best possible results. The atomisation process with which these powders are manufactured, be it water, gas or plasma atomisation, should be adapted to yield even finer powders.

When all the quantifiable parameters are considered, a prediction based on these parameters can be made with regard to the ultimate packing density of the powders. If the higher true powder density values obtained from the helium pycnometry testing are considered, it would be logical to expect a higher powder bed density from Powder B due to the significantly lower D_{90} values. Powder B, having the smallest large particles and the highest density, should lead to the highest packing density in the powder bed. Theoretically, Powder C should yield the lowest powder bed density of the three powders under investigation as it has the largest D_{10}, D_{50} and D_{90} values and is only 1.6% less dense than Powder A.

In the measurements performed, Powder A yielded the highest powder bed density, contradictory to what would be expected if all the quantifiable parameters had an equal role in the packing density. It is evident from the experimental results that the dominating factor in packing density is the minimum particle size present in the powder. With Powder A having a D_{10} value of 82% and 28,6% smaller than Powder C and Powder B, respectively, it allows Powder A to pack significantly more densely in the powder bed than any other powder under investigation. The small particles in Powder A move into the voids between the larger particles and this resulted in a 5.1% higher packing density on average.

The ratio of the larger particles to the smaller particles provides a good indication of the possible packing density of the powder in the AM unit. Both Powder B and Powder C yielded ratios of 2.56 and 2.57, respectively; Powder A, with very small particles, significantly outperforms the other two powders with a ratio of 3.94. It can be concluded that the higher the D_{90} to D_{10} ratio on particle diameter, the more densely the powder can pack in an AM unit.

Many studies in the literature are focused on the development of laser parameters within the AM units to obtain parts with high density and uniform mechanical properties. However, this is valid if little to no control is applied to the powders obtained for the manufacturing process. Only limited success will be possible when identifying the most advantageous process parameters.

3.6 Conclusion

This study investigated the powder characteristics of various commercially available laser-based powder bed fusion CoCrMo powders to determine and quantify the effect each parameter has on the packing density of the powder in the AM unit. Three different gas-atomised powders were evaluated regarding their chemical composition, particle size distribution, powder morphology, true powder density and packing density in a commercial AM unit. Manufacturing medical and dental components from CoCrMo alloy inside an AM unit is only viable if the parts produced have minimal to no porosity with repeatable and predictable mechanical properties (Saha and Roy, 2022).

The following conclusions can be drawn from this study:

- A significant variation in true powder density is present for different powders that adhere to the same standard. More

heavy elements present in the alloy and internal powder porosity could lead to this variation.

- The ICP-OES processes to determine the chemical composition of metallic powders used in the AM process have difficulty in the detection of trace elements, and MIP-OES could yield better results in future.
- Powders with small D_{90} values and high true powder density do not result in high packing densities in the AM units. Although both parameters are advantageous for high packing density, D_{10} values play a more significant role in packing density.
- Powder morphology plays the most significant role in the packing density of the powder bed. The greater the number of fine particles present, with low D_{10} values, the higher the bed density tends to be. Powders with a high D_{90} to D_{10} ratio would lead to the highest packing density.

This work highlights the relationship between the particle size distribution and the powder bed packing density inside an AM unit. The recoating unit's layer-by-layer application of the powder to the powder bed does not ensure the tightly packed powder particles that could be achieved by powder agitation. The originality of this work is in determining and quantifying the factors that affect the packing density of the powder in the powder bed. The implication of this research for industrial and research applications is the ability to define and quantify the most important parameters when a powder is procured. Deciding on parameters such as particle size distribution and powder morphology could lead to higher-quality parts produced by laser-based powder bed fusion units.

References

Abdulhameed, O., Al-Ahmari, A., Ameen, W. and Mian, S.H. (2019), "Additive manufacturing: challenges, trends, and applications", *Advances in Mechanical Engineering*, Vol. 11 No. 2.

ASTM (2017), "ASTM standard B311-17", ASTM.org.

Auricchio, F. and Marconi, S. (2016), "3D printing: clinical applications in orthopaedics and traumatology", *EFORT Open Reviews*, Vol. 1 No. 5, pp. 121-127.

Averardi, A., Cola, C., Zeltmann, S.E. and Gupta, N. (2020), "Effect of particle size distribution on the packing of powder beds: a critical discussion relevant to additive manufacturing", *Materials Today Communications*, Vol. 24, p. 100964.

Bai, S.-W., Mei, H., Zhang, M.-G., Zhou, S.-X., Yan, Y.-K., Cheng, L.-F., Zhang, L.-T. and Lu, J. (2023), "3D printing assemble technology toward advanced photocatalysis", *Materials Today Nano*, Vol. 24, p. 100385.

Cacace, S. and Semeraro, Q.A.M. (2020), "Influence of the atomization medium on the properties of stainless steel SLM parts", *Additive Manufacturing*, Vol. 36, p. 101509.

Einhauser, T.J. (1997), "ICP-OES and SEM-EDX analysis of dust and powder produced by the laser-processing of a Cr-Ni-Steel alloy", *Mikrochemica Acta*, Vol. 127, pp. 265-268.

Fontoura, B.M., Jofré, F.C., Williams, T., Savio, M., Donati, G.L. and Nóbrega, J.A. (2022), "Is MIP-OES a suitable alternative to ICP-OES for trace element analysis?", *Journal of Analytical Atomic Spectrometry*, Vol. 37 No. 5, pp. 966-984.

Hu, K., Zhou, Y., Sitaraman, S.K. and Tentzeris, M.M. (2023), "Additively manufactured flexible on-package phased array antennas for 5G/mm wave wearable and conformal digital twin and massive MIMO applications", *Scientific Reports*, Vol. 13 No. 1, p. 12515.

Jacob, G., Donmez, A., Slotwinski, J. and Moylan, S. (2016), "Measurement of powder bed density in powder bed fusion additive manufacturing processes", *Measurement Science and Technology*, Vol. 27 No. 11, p. 115601.

Saha, S. and Roy, S. (2022), "Metallic dental implants wear mechanisms, materials, and manufacturing processes: a literature review", *Materials (Basel)*, Vol. 16 No. 1, p. ma16010161.

Shinde, M.S. and Ashtankar, K.M. (2017), "Additive manufacturing–assisted conformal cooling channels in mold manufacturing processes", *Advances in Mechanical Engineering*, Vol. 9 No. 5.

Slotwinski, J.A. and Garboczi, E.J.J.J. (2015), "Metrology needs for metal additive manufacturing powders", *JOM*, Vol. 67 No. 3, pp. 538-543, available at: https://link.springer.com/article/10.1007/s11837-014-1290-7

Spierings, A.B., Herres, N. and Levy, G.J.R.P.J. (2011), "Influence of the particle size distribution on surface quality and mechanical properties in AM steel parts", *Rapid Prototyping Journal*, Vol. 17 No. 3, available at: http://utw10945.utweb.utexas.edu/Manuscripts/2010/2010-33-Spierings.pdf

Tan, J.H., Wong, W.L.E. and Dalgarno, K.W. (2017), "An overview of powder granulometry on feedstock and part performance in the selective laser melting process", *Additive Manufacturing*, Vol. 18, pp. 228-255.

Townsend, A., Senin, N., Blunt, L., Leach, R.K. and Taylor, J. S. (2016), "Surface texture metrology for metal additive manufacturing: a review", *Precision Engineering*, Vol. 46, pp. 34-47.

Zhang, H., Prasad Vallabh, C.K. and Zhao, X. (2023), "Machine learning enhanced high dynamic range fringe projection profilometry for in-situ layer-wise surface topography measurement during LPBF additive manufacturing", *Precision Engineering*, Vol. 84, pp. 1-14.

Zhao, Z., Wang, J., Du, W., Bai, P. and Wu, X. (2023), "Numerical simulation and experimental study of the 7075 aluminum alloy during selective laser melting", *Optics & Laser Technology*, Vol. 167, p. 109814.

Further reading

Ahangar, P., Cooke, M.E., Weber, M.H. and Rosenzweig, D. H. (2019), "Current biomedical applications of 3D printing and additive manufacturing", *Applied Sciences*, Vol. 9 No. 8, p. app9081713.

Hoque, M.E., Showva, N.N., Ahmed, M., Rashid, A.B., Sadique, S.E., El-Bialy, T. and Xu, H. (2022), "Titanium and titanium alloys in dentistry: current trends, recent

developments, and future prospects", *Heliyon*, Vol. 8 No. 11, p. e11300.

Nouri, A., Rohani Shirvan, A., Li, Y. and Wen, C. (2021), "Additive manufacturing of metallic and polymeric load-bearing biomaterials using laser powder bed fusion: a review", *Journal of Materials Science & Technology*, Vol. 94, pp. 196-215.

Strondl, A., Lyckfeldt, O., Brodin, H. and Ackelid, U. (2015), "Characterization and control of powder properties for additive manufacturing", *JOM*, Vol. 67 No. 3, pp. 549-554.

Corresponding author

Cornelius P. Kloppers can be contacted at: cp.kloppers@nwu.ac.za